



Circadian circuits in humans

Koller, Kristin; Rafal, Robert D; Mullins, Paul G

Cortex

DOI:

[10.1016/j.cortex.2019.01.011](https://doi.org/10.1016/j.cortex.2019.01.011)

Published: 01/01/2020

Peer reviewed version

[Cyswllt i'r cyhoeddiad / Link to publication](#)

Dyfyniad o'r fersiwn a gyhoeddwyd / Citation for published version (APA):

Koller, K., Rafal, R. D., & Mullins, P. G. (2020). Circadian circuits in humans: White matter microstructure predicts daytime sleepiness. *Cortex*, 122, 97-107.
<https://doi.org/10.1016/j.cortex.2019.01.011>

Hawliau Cyffredinol / General rights

Copyright and moral rights for the publications made accessible in the public portal are retained by the authors and/or other copyright owners and it is a condition of accessing publications that users recognise and abide by the legal requirements associated with these rights.

- Users may download and print one copy of any publication from the public portal for the purpose of private study or research.
- You may not further distribute the material or use it for any profit-making activity or commercial gain
- You may freely distribute the URL identifying the publication in the public portal ?

Take down policy

If you believe that this document breaches copyright please contact us providing details, and we will remove access to the work immediately and investigate your claim.

Circadian circuits in humans: White matter microstructure predicts daytime sleepiness

1 *Kristin Koller^{1,2}, Robert D. Rafal^{1,3} & Paul G. Mullins¹*

2 ¹ *Wolfson Centre for Clinical and Cognitive Neuroscience, School of Psychology, Bangor*
3 *University, Bangor, Gwynedd, United Kingdom*

4 ² *Cardiff University Brain Research Imaging Centre (CUBRIC), Cardiff University, Cardiff,*
5 *United Kingdom*

6 ³ *Department of Psychological and Brain Sciences, University of Delaware, Delaware,*
7 *United States of America*

8

9 Corresponding author at: Cardiff University Brain Research Imaging Centre (CUBRIC),
10 Cardiff University, Cardiff, United Kingdom. E-mail address: kollerk@cardiff.ac.uk (K.
11 Koller). Research was conducted at Wolfson Centre for Clinical and Cognitive Neuroscience,
12 School of Psychology, Bangor University, Bangor, Gwynedd, United Kingdom.

13 **Abstract**

14

15 The suprachiasmatic nucleus of the hypothalamus is the chief circadian pacemaker in the
16 brain, and is entrained to day-night cycles by visual afferents from melanopsin containing
17 retinal ganglion cells via the inferior accessory optic tract. Tracer studies have demonstrated
18 efferents from the suprachiasmatic nucleus projecting to the paraventricular nucleus of the
19 hypothalamus, which in turn project to first-order sympathetic neurons in the intermedio-
20 lateral grey of the spinal chord. Sympathetic projections to the pineal gland trigger the
21 secretion of the sleep inducing hormone melatonin. The current study reports the first
22 demonstration of potential sympathopetal hypothalamic projections involved in circadian
23 regulation in humans with *in vivo* virtual white matter dissections using probabilistic
24 diffusion tensor imaging (DTI) tractography. Additionally, our data shows a correlation
25 between individual differences in white matter microstructure (measured with fractional
26 anisotropy) and increased daytime sleepiness (measured with the Epworth Sleepiness Scale
27 (ESS, Johns, 1991)). Sympathopetal connections with the hypothalamus were virtually
28 dissected using designated masks in the optic chiasm, which served as an anatomical
29 landmark for retinal fibres projecting to the suprachiasmatic nucleus, and a waypoint mask on
30 the lateral medulla, where hypothalamic projections to the sympathetic nervous system

31 traverse in humans. Sympathopetal projections were demonstrated in each hemisphere in
32 twenty-six subjects. The tract passed through the suprachiasmatic nucleus of the
33 hypothalamus and its trajectory corresponds to the dorsal longitudinal fasciculus traversing
34 the periaqueductal region and the lateral medulla. White matter microstructure (FA) in the
35 left hemisphere correlated with high scores on the ESS, suggesting an association between
36 circadian pathway white matter microstructure, and increased daytime sleepiness and
37 decreased arousal.

38

39 Keywords: suprachiasmatic nucleus, diffusion tensor imaging, melatonin, circadian rhythms,
40 sleep-wakefulness.

1 Circadian rhythms are biochemical, physiological and behavioural rhythms that oscillate with
2 a period close to 24 hours and are generated via an internal pacemaker, the suprachiasmatic
3 nucleus of the hypothalamus, located in the rostroventral hypothalamus above the optic
4 chiasm (Fuller & Fuller, 2002). The suprachiasmatic nucleus is considered to be the chief
5 pacemaker for clock genes in the brain in addition to regulating various endocrine,
6 physiological and behavioural circadian rhythms (Hoffmann & Swaab, 1993). Circadian
7 rhythms have been demonstrated in diurnal cycles of core body temperature, and the release
8 of hormones such as melatonin and cortisol (Hoffstra & de Weerd, 2008).

9

10 While this characteristic near 24-hour cycle persists in the absence of environmental time-
11 cues (e.g. light), daylight acts as a *zeitgeber* to ensure that it is entrained to the light-dark
12 solar cycle (Fuller & Fuller, 2002). Light signals transduced by melanopsin containing retinal
13 ganglion cells (Gooley et al., 2001) are transmitted to the suprachiasmatic nucleus via the
14 inferior accessory optic tract (Moore et al., 1966). This circuitry allows entrainment of the
15 suprachiasmatic nucleus, which regulates the sleep-wake cycle through the sleep inducing
16 hormone melatonin, to light-dark cycles.

17

18 Light induced inhibition of melatonin secretion is controlled through a multi-synaptic
19 pathway from the suprachiasmatic nucleus to the pineal gland (Moore & Card, 1986;
20 Teclemariam-Mesbah et al., 1999). The suprachiasmatic nucleus projects to the
21 paraventricular nucleus including its autonomic parts such as the dorsal paraventricular
22 nucleus (pe) and the medial parvocellular part (mp). Direct hypothalamic projections from
23 the paraventricular nucleus in turn synapse in the intermediolateral column in the first
24 segment of the thoracic spinal cord, where first order sympathetic neurons further project to
25 the superior cervical ganglion. Second order sympathetic fibres project from the superior
26 cervical ganglia to the pineal gland (Kappers, 1976). Sympathetic fibres reach the pineal
27 gland, entering the apex of the pineal gland from the region of the *tentorium cerebelli* as
28 single or paired *nervi conarii* in humans and rodents. Norepinephrine is released from their
29 terminals forming synapses on the surface of pinealocytes, which thereby convert serotonin
30 into melatonin (Alarma-Estrany & Pintor, 2007). A schematic presentation of this pathway is
31 presented in Figure 1. Our study set out to visualise the descending, sympathopetal
32 component of these hypothalamic projections in human volunteers, and to examine how the
33 microstructure of this pathway may relate to measures of circadian rhythm.

34

1 To do so, we used probabilistic DTI tractography to virtually dissect potential descending
2 pathways that may function in regulating diurnal sleep-wake cycles. Our goal was to
3 demonstrate hypothalamic projections to the sympathetic nervous system that receive
4 afferents from the suprachiasmatic nucleus. The chief circadian pacemaker is termed
5 suprachiasmatic, due to its location directly dorsal to the optic chiasm. Since it is small and
6 its margins are not discernable on MRI images, it was not possible to reliably draw a seed
7 mask that was restricted to the suprachiasmatic nucleus. Therefore, to ensure that the
8 connection passed through the suprachiasmatic nucleus, a seed mask was drawn on the optic
9 chiasm (from which the suprachiasmatic nucleus receives visual afferents). A waypoint mask
10 was drawn on the lateral medulla, through which hypothalamic projections to the
11 sympathetics are known to pass (Naidich et al., 2009). Connections between the
12 suprachiasmatic nucleus and the lateral medulla were virtually dissected in two groups of
13 sleep-chronotype individuals; morning and evening types. Individual differences in
14 microstructure (using fractional anisotropy) of the resulting pathways, in addition to
15 physiological measures of circadian rhythms (melatonin, cortisol, heart rate, breathing rate
16 and temperature) were compared between morning and evening sleep types. We successfully
17 demonstrated the posited pathway and provide novel evidence that, although the
18 microstructure of the proposed sympathetic sleep circuit dissected in our sample did not
19 correlate with measures of circadian rhythms, its microstructure (FA) did predict daytime
20 sleepiness.

21

22 Our prediction was that measures of circadian rhythm would correlate with microstructure of
23 virtual dissections of the proposed sleep pathway. However, instead, our data shows that
24 daytime sleepiness correlated with microstructure of the sleep pathway. Therefore, we
25 conclude that the strong correlation between microstructure of the sleep pathway and daytime
26 sleepiness offers only evidence for the functional veracity of its role in sleep, but not a
27 putative mechanism by which this is achieved.

28

29

30

31

32

33

34

1 **Material and Methods**

2

3 **Participants**

4

5 An initial sample of 27 healthy participants (15 female, age range 21-57) was recruited from
6 the population at Bangor University. The study was advertised through posters, online forums
7 and a participant recruitment website at Bangor University. Potential participants were first
8 required to fill out the Morningness-Eveningness Questionnaire (Horne & Östberg, 1976),
9 Beck's Depression Inventory (Beck, Steer & Brown, 1996), the Epworth Sleepiness Scale
10 (Johns, 1991) and a short questionnaire on lifestyle and sleeping habits that may interfere
11 with circadian rhythms. Questionnaires were sent to participants in the form of online links
12 that were completed online to allow participants to fill out confidential information in private
13 at their own convenience. Each participant was provided with a confidential participant
14 number when filling out online questionnaires to ensure anonymity. Participants were invited
15 to take part in the study if they met the following inclusion criteria: 1) scored either as an
16 'early bird' (>58) or 'night owl' (<42) on the MEQ, 2) scored below the threshold that would
17 indicate mild to moderate depression on BDI (<9), 3) scored below the threshold that would
18 indicate excessive daytime sleepiness on the ESS (<10) and 4) demonstrated that their sleep
19 type (as indicated by MEQ score) was not due to lifestyle factors such as shift work, heavy
20 alcohol consumption, sleep disorders or use of medication. Participants had no known
21 neurological, psychological, psychiatric, sleep or cognitive impairments. Finally, participants
22 were screened against exclusion criteria related to MR safety. Monetary compensation was
23 provided for participation in MRI scanning. One participant was excluded from the study
24 after failure to adhere to the study instructions. Ethical approval was received from Bangor
25 University's Ethics Review Committee and prior written consent was obtained from all
26 participants. This study conformed to the ethical standards of the Declaration of Helsinki.
27 Participants were informed that their data and personal demographical information would be
28 kept anonymous at all times.

29

30

31

32

33

34

1 **MRI data collection and pre-processing protocol**

2

3 **Magnetic resonance scanner**

4

5 All imaging data was collected on a Phillips 3 Tesla Achieva magnetic resonance (MR)
6 scanner (Phillips Medical, Best, Netherlands) at the Bangor Imaging Unit at Bangor
7 University.

8

9 **T1 anatomical scans**

10

11 High resolution multi-echo T1 weighted images (0.7x0.7x0.7 mm isotropic voxel resolution)
12 were acquired using a 5 echo averaged MP-RAGE sequence (TE = 3.5, 5.1, 6.8, 8.5, 10.2 ms,
13 effective TE = 6.7 ms, TR = 12 ms, TI = 1150 ms, 3D acquisition, FOV = 240 mm X 220
14 mm X 130 mm, voxel dimensions = 0.7 X 0.7 X 0.7 mm³).

15

16 **DTI scans**

17

18 DWI-EP (diffusion weighted imaging – echo planar) images were collected at 2x2x2mm with
19 the following parameters: b-values = 0 (averaged four volumes) and 2000, b-directions = 61,
20 slices = 76, section thickness = 2mm, TR = 2 s, TE = 35ms. All participants were scanned
21 using a 32-channel head coil.

22

23 **MRI Data pre-processing**

24

25 Following data acquisition, the image files for the DTI data and the structural T1 scans were
26 manually converted from DICOM format into NIFTI with dcm2nii
27 (<http://www.sph.sc.edu/comd/rorden/mricron/>). Subsequent data pre-processing was carried
28 out using the FSL-FDT toolbox (Behrens et al, 2003, 2007;
29 <http://fsl.fmrib.ox.ac.uk/fsl/fslwiki/>). Diffusion weighted images were corrected for eddy
30 currents and head motion using affine registration to the first b-zero volume. This was carried
31 out to prevent approximate stretches and shears created in the diffusion weighted images that
32 may have been induced by eddy currents in the gradient coils (Behrens et al., 2007). After
33 eddy current correction, diffusion tensor models were fitted at each voxel using the DTI-FIT
34 tool in FSL. Diffusion parameters were calculated using the Markov Chain Monte Carlo

1 sampling method. The DTI data was then prepared for probabilistic tractography via the
2 BEDPOSTX tool in FSL's FDT toolbox. BEDPOSTX ran with the following parameters:
3 number of fibres modelled per voxel = 3, weight = 1, burning period = 2000).
4 Probabilistic tracking was carried out using the PROBTRACKX tool in FSL's FDT toolbox.
5 PROBTRACKX ran with the following parameters: curvature threshold = .02, number of
6 samples generated per voxel = 5000, number of steps per sample = 2000 and steplength =
7 .05. Prior to running the BEDPOSTX process, the non-diffusion brain image was extracted
8 from the skull (using the FSL brain extraction tool (BET)), and a brain mask was formed.
9 Anatomical T1-weighted scans were brain extracted using the BET-tool, and were registered
10 with the B0 diffusion brain image, using FSL's FLIRT tool. Masks were drawn based on
11 anatomical landmarks in each participant's individual non-diffusion T1-registered brain using
12 FSLView.

13

14 **Physiological measures of circadian rhythms**

15

16 Participants additionally provided physiological measures of circadian rhythms including
17 saliva samples to test for melatonin, and measures of heart rate, breathing rate and
18 temperature. In accordance with the Salimetrics ® saliva collection protocol, participants
19 were required to abstain from consuming alcohol, caffeine, nicotine, strenuous exercise,
20 aspirin and ibuprofen during the testing period. Participants were asked to adhere to these
21 restrictions from the evening prior to the testing day until after the final saliva sample was
22 collected. Consumption of food was allowed only up until 30 minutes prior to saliva
23 collection. One participant was excluded from the study after failure to adhere to the study
24 instructions. Heart rate was measured by asking the participant to count the number of pulse
25 beats on their wrist for one minute. Breathing rate was measured as the amount of breaths
26 (one breath counted as one inhale and one exhale) per minute. Disposable oral thermometers
27 were used to measure body temperature. In comparison to circadian hormones (melatonin and
28 cortisol) and temperature, measured via physiologically robust saliva sample assay and oral
29 thermometers, respectively, measures of heart and breathing rate were self counted, but under
30 thorough supervision by the experimenter. Therefore, measures of heart and breathing rate
31 should be considered less rigorous as measures of circadian rhythm.

32

33

34

1 **Procedure**

2

3 Physiological measures were carried out in the morning (8am) and evening (9pm) on the
4 same day as MRI testing. All MRI data collection was conducted during morning hours
5 (9am-12am). Participants had the option to collect the measures in the privacy of their own
6 home, or to receive assistance from the experimenter at Bangor University. Following the
7 Salimetrics ® saliva collection protocol, ten minutes prior to saliva collection, the participant
8 was required to rinse orally with water only and was asked to sit still in a darkened room with
9 minimal light (<8 Lux). After 10 minutes, participants collected their own saliva sample in a
10 cryovial tube. Tubes were labelled and coded to ensure anonymity, and were immediately
11 stored in a freezer in a Human Tissue Authority licensed lab (at approximate temperature -20
12 °C) at Bangor University. Following saliva collection, the participant was provided with a
13 disposable thermometer and asked to place it under the tongue for 60 seconds. The
14 participant was then asked to locate their pulse on their wrist and count the number of beats
15 per minute, over one minute. Finally, the number of breaths per minute was recorded. The
16 experimenter recorded the times of saliva, temperature, heart rate and breathing rate
17 collection to ensure that the timings were the same for each participant. Prior to MRI
18 scanning, the participant was provided with a MRI safety-screening questionnaire and
19 interview. Once both the experimenter and the participant were satisfied that it was safe for
20 the participant to be scanned, the scanning session started and lasted approximately 40
21 minutes.

22

23 **Virtual dissection of sleep pathways with probabilistic DTI tractography**

24

25 **Probabilistic tractography**

26

27 The goal of the virtual dissection was to generate connections that traversed the
28 suprachiasmatic nucleus of the hypothalamus through the lateral medulla en route to the
29 sympathetic nervous system in the spinal cord. To demonstrate such hypothalamic
30 projections from the paraventricular nucleus neurons that receive afferents from the
31 suprachiasmatic nucleus, a seed mask was placed in the optic chiasm from which visual
32 afferents project to the suprachiasmatic nucleus via the inferior accessory optic tract. A
33 waypoint mask was placed on the lateral medulla to visualize projections from the
34 paraventricular nucleus of the hypothalamus that synapse on preganglionic first order

1 sympathetic neurons in the intermediolateral column of the spinal cord.

2

3 Connections were generated using FSL's FDT DIFFUSION toolbox in PROBTRACKX
4 (Behrens et al., 2003; Behrens, Johansen-Berg, Jbabdi & Woolrich, 2007) in both
5 hemispheres of each subject's diffusion weighted image using the subject-specific masks
6 manually drawn on: 1) the optic chiasm, 2) the lateral medulla and 3) exclusion regions.
7 Masks were drawn manually (using FSL's FSLVIEW in the FDT DIFFUSION toolbox) on
8 each subject's diffusion space registered T1-weighted anatomical brain image using FSL's
9 FLIRT LINEAR REGISTRATION). Figure 2 shows the optic chiasm and lateral medulla
10 region of interest masks, in addition to an exclusion mask in one representative subject.

11

12 The value of each voxel of the resulting connection represented the total number of traces
13 passing through that voxel. We thresholded each voxel so that only voxels that contained at
14 least 10% of the maximum number of traces found in any voxel remained. A study that
15 directly compared diffusion tensor imaging (DTI) tractography with tracers in monkeys has
16 reported that a threshold of 10% is optimal to most reliably reflect the anatomy of
17 tractography compared with tracers (Azadbakht et al. 2015). Connections were generated in
18 both directions (i.e. optic chiasm as seed and lateral medulla as waypoint mask, and vice
19 versa). The two connections generated in each hemisphere were added together (using
20 FSLMATHS), and only voxels that 'overlapped', i.e. were present in both connections, were
21 isolated as a composite connection in each hemisphere of each participant for use as a mask
22 in subsequent analyses of white matter microstructure.

23

24

25 **Measurement of FA values and statistical analyses**

26

27 Voxels in the composite overlap connection in each hemisphere of each participant were used
28 as masks in native diffusion space to calculate, with FSLmaths, the mean fractional
29 anisotropy values of all voxels in each connection for each participant. The composite
30 overlap of the voxels that were present only in connections in both directions were isolated in
31 order to include voxels that would most likely be part of the neural pathway between the
32 suprachiasmatic nucleus and the lateral medulla. We presumed that voxels containing fibres
33 regulating circadian rhythms could also include other fibers projecting from the
34 paraventricular nucleus to the sympathetic nervous system. Since the structural connectivity

1 of these non-circadian projections were presumed to have no correlation with sleep
2 behaviour, it was important to reduce noise by constraining the size of the connection as
3 much as possible and to exclude, as much as possible, other projections to the sympathetics in
4 the spinal cord, in addition to other adjacent descending tracts in the densely packed
5 brainstem.

6
7 For visualization purposes, and for demonstration of anatomical variability across
8 participants, composite, binarized connections for all participants were registered to the same
9 brain space and added together to produce images showing the percent of participants
10 through which the connection passed in each voxel (Figure 3).

11
12

13 **Statistical analyses**

14

15 The first goal of this study was to virtually dissect a connection between the suprachiasmatic
16 nucleus of the hypothalamus and the lateral medulla using diffusion tensor tractography.

17 The second goal was to test for behavioural and physiological differences between
18 morning and evening sleep type individuals. To simplify this comparison of several sleep and
19 circadian rhythm measures, a single score was computed for each measure (mean
20 concentration of melatonin in pg/ml, and measures of temperature, heart rate and breathing
21 rate) by subtracting the score obtained in the evening testing from that obtained in the
22 morning testing for each participant. Independent samples t-tests were carried out to compare
23 scores of measures of 1) mean concentration of melatonin, 2) temperature, 3) heart rate, 4)
24 breathing rate and 5) white matter microstructure (FA) of the dissected connection between
25 the suprachiasmatic nucleus and the lateral medulla (FA) between morning and evening sleep
26 types. In order to control for multiple comparisons, Bonferroni correction for multiple
27 comparisons was carried out.

28 The final goal of this study was to attempt to validate that the pathway we dissected
29 with DTI plays a function in regulating sleep. In order to achieve this, mean FA values of the
30 resulting overlap sleep pathways were correlated with measures of sleep behaviour (salivary
31 melatonin and daytime sleepiness) across participants. Firstly, a paired samples t-test was
32 employed to test for differences in FA between dissected pathways in the left and right
33 hemispheres. Pearson correlation was used to test for correlations between microstructure
34 between the suprachiasmatic nucleus and the lateral medulla (FA) and two measures of sleep:

1 1) melatonin and 2) scores on daytime sleepiness (ESS scores) for each participant in the left
2 and right hemispheres. Bonferonni correction for multiple comparisons was carried out for
3 correlations between pathway FA and 1) melatonin and 2) ESS scores for both the left and
4 right hemispheres.

5 6 **Results**

7 8 **Virtual dissection between the suprachiasmatic nucleus and the lateral medulla with** 9 **probabilistic DTI tractography**

10
11 Virtual dissection of tracts connecting the suprachiasmatic nucleus of the hypothalamus to
12 the lateral medulla were demonstrated bilaterally in 24 participants, and unilaterally in the
13 left hemisphere of one participant and the right hemisphere of another. One participant did
14 not demonstrate the pathway either in the left or the right hemisphere. This connection
15 demonstrates a putative sympathopetal circadian pathway from the hypothalamus that
16 traverses the paraventricular nucleus of the hypothalamus to the intermediolateral column in
17 the spinal cord. Its trajectory connects retino-hypothalamic fibres in the inferior accessory
18 optic tract to the suprachiasmatic nucleus, passes through the paraventricular nucleus of the
19 hypothalamus and thence follows a trajectory corresponding to the dorsal longitudinal
20 fasciculus of Schütz which traverses the dorsal midbrain through the periaqueductal region.

21
22 For illustration purposes, Figure 3 presents the common overlap of the composite connection
23 from all participants registered to a common brain space. However, as described below, mean
24 FA was calculated for each individual in each hemisphere in native diffusion space.

25 26 **Calculation of microstructure with fractional anisotropy**

27
28 Overlapped tracts for each participant were used as masks on the fractional anisotropy (FA)
29 image for each participant (generated with DTIFIT utility in the FTD toolbox of FSL) to
30 calculate mean FA values for each connection in each individual participant. Paired-samples
31 t-tests demonstrated no significant differences in mean FA between left and right pathways (t
32 (23) = -.78, $p = .44$, two-tailed). Table 1 presents FA values of the connection for each
33 participant.

1 **Differences between morning and evening sleep types**

2
3 An independent samples t-test demonstrated no significant differences in the mean FA
4 averaged across the left and right hemispheres for each participant (a single hemisphere value
5 was used in place of an average for participants in whom the tract was demonstrated in one
6 hemisphere only) between the morning and evening sleep type groups ($t(24) = .55, p = .59$).
7 In order to compare physiological results between the groups of morning and evening sleep
8 types, new scores were computed for each measure by subtracting the score that was obtained
9 in the evening testing from the morning testing. Difference scores were computed for the
10 mean concentration of melatonin in pg/ml, and measures of temperature, heart rate and
11 breathing rate. Independent samples t-tests showed no significant differences in melatonin
12 ($t(21) = -1.68, p = .12$), cortisol ($t(22) = 1.72, p = .1$), breathing rate ($t(22) = 1.68, p = .11$ or
13 heart rate ($t(22) = 1.56, p = .13$) between the two sleep groups. A significant difference was
14 obtained for temperature between morning and evening types ($t(23) = 2.58, p = .017$) with a
15 larger temperature decrease demonstrated for the evening type group. However, this result
16 did not survive the significance cut off of $p < .002$ after Bonferroni correction for multiple
17 comparisons. Figure 4 presents bar graphs and difference scores between morning and
18 evening type sleep groups.

21 **Microstructure of suprachiasmatic nucleus – lateral medulla tract with measures of** 22 **sleep behaviour**

23
24 Microstructure (FA) between the suprachiasmatic nucleus and the lateral medulla were
25 correlated with two measures of sleep; 1) melatonin measures and scores on daytime
26 sleepiness as measured by the ESS. Pearson correlation demonstrated no significant
27 correlation between FA of the suprachiasmatic nucleus – lateral medulla connections and
28 mean melatonin difference scores (i.e the amount of diurnal fluctuation in melatonin levels)
29 in the left hemisphere ($r = .3, p = .17, N = 22$) or the right hemisphere ($r = -.05, p = .83, N =$
30 22). Furthermore, no correlations were observed for total melatonin measured (morning and
31 evening measures added) and pathway microstructure in the left ($r = .23, p = .28$) or the right
32 ($r = -.07, p = .76$) hemispheres. A significant correlation was observed between FA of
33 connections in the left hemisphere and daytime sleepiness as measured by the ESS ($r = .69, p$
34 $< .001, N = 25$) (Figure 5). No significant correlation was observed between daytime

1 sleepiness and FA in the right hemisphere ($r = .18, p = .39, N = 25$). The effect of FA in the
2 left hemisphere to predict daytime sleepiness was significant after Bonferroni correction for
3 multiple comparisons ($p < .002$). Correlations between microstructure (FA) in the left and
4 right were not significant in any of the other measures of circadian rhythm.

5

6 **Critical consideration of plausibility of virtually dissected pathway**

7

8 Considering the challenges inherent to probabilistic tractography, we carried out several quality
9 assurance checks to rule out potential false positives for the virtually dissected sleep tracts.
10 Data quality assessment was carried out to ensure that none of the diffusion images were
11 subjected to distortions in the region of the optic chiasm. Although distortions are likely to
12 exist in all areas throughout the brain, bias field distortions are likely to be more extensive in
13 orbitofrontal regions, and although this region is in close proximity to the optic chiasm, our
14 data suggest that this area was unaffected by bias field distortions (Figure 6.) Furthermore,
15 although the seed mask was placed in the optic chiasm, the tract connects in the direction
16 opposite to the orbitofrontal region, thus making the possibility of obtaining the tract as a result
17 of false positive connections due to bias field distortion unlikely. To ensure that the region of
18 interest masks overlapped with the correct corresponding anatomical landmarks, several quality
19 assessment steps were carried out to ensure that the masks corresponded with the DTI data. The
20 T1 structural image was first registered to the diffusion brain, and the masks were drawn on
21 this registered image. Thus, the masks were drawn in diffusion space with the T1 structural
22 registered to diffusion space as an anatomical guide. Furthermore, the masks were then
23 overlaid on the B0 diffusion image to confirm that the masks matched to local anatomical
24 landmarks in diffusion space. Additionally, visualisation of the tensor model in close up along
25 the tract close to seed regions demonstrated that the direction in each voxel were consistent
26 along the tract (Figure 7). Together, the data quality checks above suggest that the virtually
27 dissected tracts were unlikely to have been demonstrated due to spurious connections
28 influenced by distortion.

29

1 **Discussion**

2

3 **Summary of main findings**

4

5 In this study, descending white matter pathways postulated to be involved in the regulation of
6 circadian rhythms were virtually dissected in the human brain with the use of probabilistic
7 diffusion tensor imaging tractography. Seed masks were placed in the optic chiasm to ensure
8 that the resultant connections would demonstrate connections between the suprachiasmatic
9 nucleus of the hypothalamus, the chief internal circadian pacemaker, which is located directly
10 above the optic chiasm and which receives retinal afferents via the inferior accessory optic
11 tract. The resulting connections passed through the region of lateral medulla known to
12 transmit hypothalamic projections, originating in the paraventricular nucleus, to pre-
13 ganglionic sympathetic neurons in the intermediolateral column of the spinal cord. Its
14 topography was visualized as a flat trajectory across the meso-diencephalic junction and then
15 descended along the midline through the periaqueductal region to the lateral medulla. The
16 trajectory demonstrated in these virtual dissections corresponds to the anatomy of the dorsal
17 longitudinal fasciculus of Schütz (1891), which contains sympathopetal fibers projecting
18 from parvocellular neurons in the paraventricular nucleus of the hypothalamus to first order
19 preganglionic neurons in the intermediolateral gray column of the spinal cord (Kiernan,
20 2005).

21

22 Comparison of measures of circadian rhythms between morning compared to evening type
23 groups demonstrated no differences in measures of heart rate, melatonin, cortisol, breathing
24 rate and microstructure (FA) of the connections between the suprachiasmatic nucleus and
25 lateral medulla. However, a trend of greater temperature difference between morning and
26 evening measures were observed within the evening type group compared to the morning
27 type group. White matter microstructure of the circadian tract in the left hemisphere predicted
28 daytime sleepiness as measured by the Epworth Sleepiness Scale (Johns, 1991). However no
29 correlations between pathway microstructure and diurnal fluctuations of salivary melatonin
30 was observed. Findings from this study indicated that the microstructure of the virtually
31 dissected pathway connecting the suprachiasmatic nucleus and lateral medulla in the left
32 hemisphere plays a role in modulating sleep-wakefulness.

33

34

1 **Anatomical connectivity**

2

3 Tracer studies in several species have shown that there are direct, sympathopetal projections
4 from the paraventricular nucleus of the hypothalamus that synapse on pre-ganglionic, first
5 order sympathetic neurons in the intermediolateral column of the spinal cord (Cechetto &
6 Saper, 1988, Larsen et al., 1991; Hosoya et al.,1985). There is evidence that these
7 sympathopetal fibers descend through two distinct pathways (Larsen et al, 1998): one
8 coursing along the periaqueductal gray and another through the central pons (Swanson, 1977,
9 Figure 5, p. 351). In humans, the pathway passing through the periaqueductal region is a
10 component of the dorsal longitudinal fasciculus (Kiernan, 2005).

11 It has not been previously established which of these descending hypothalamo-sympathetic
12 pathways contain fibers from the hypothalamus that transmit signals from the
13 suprachiasmatic nucleus to regulate circadian cycles through sympathetic efferents to the
14 pineal gland. The ‘classical model’ of neural control of the pineal (Larsen et al., 1998, Figure
15 1, p. 129) depicts these axons as traversing the centre of the pons.

16

17 However, Larsen et al. (1998) specifically examined hypothalamic connections to
18 sympathetic neurons in the intermediolateral column of the spinal cord that were involved in
19 control of pineal gland secretion. They injected a neurotropic alpha herpesvirus (pseudorabies
20 virus) into the pineal gland of rats, and localized viral antigens in infected neurones at various
21 postinoculation intervals. Infected neurons were observed in the superior cervical ganglion,
22 intermediolateral column of the thoracic spinal cord, periaqueductal gray, and the
23 paraventricular and suprachiasmatic nuclei of the hypothalamus.

24

25 In the current study, we attempted to identify the descending sympathopetal projections from
26 the hypothalamus that transmitted signals from the central circadian pacemaker, the
27 suprachiasmatic nucleus of the hypothalamus. The human pathway demonstrated in the
28 current study traversed the periaqueductal region as a component of the sympathopetal fibers
29 in the dorsal longitudinal fasciculus. This topography is consistent with the trajectory
30 described by Larsen et al. (1998) in rats. Circadian circuitry mediates a primitive function, so
31 it might be expected to be highly conserved during evolution.

32

33 Tractography did not demonstrate hypothalamic connections to the sympathetic nervous
34 system that project in the more ventral pathway through the central pontine tegmentum. Since

1 the seed mask used was the optic chiasm, it is possible that the connection passed through
2 just the part of the paraventricular nucleus that projects through the dorsal longitudinal
3 fasciculus. Given the low spatial resolution of diffusion imaging, however, it seems unlikely
4 that some of the voxels through which the connection passed did not contain fibres that
5 projected through the more ventral route in the pontine tegmentum. It is more likely that the
6 failure to demonstrate the more ventral pathway reflects a limitation of tractography.
7 Tractography demonstrates the vector of anisotropic water diffusion. It provides no
8 information about the direction of axonal projections, or synaptic connections. A connection
9 is only generated in voxels which predominantly contain axons oriented in the same
10 direction. If fibres cross within a voxel perpendicular to another, mean diffusion in that voxel
11 will not be anisotropic. Unlike the dorso-medial pons in which there are dominantly
12 longitudinally oriented fibres, the pontine tegmentum contains both longitudinal (ascending
13 and descending) fibres, and transversely oriented fibres. This may have precluded
14 demonstration of the ventral pathway through the pontine tegmentum in our virtual
15 dissection.

16

17 **Microstructure of the suprachiasmatic nucleus-lateral medulla connection in the left** 18 **hemisphere predicts daytime sleepiness**

19

20 Our results demonstrated that the white matter microstructure (FA) of the suprachiasmatic
21 nucleus-lateral medulla pathway predicted daytime sleepiness, however this effect was only
22 demonstrated in the left hemisphere. Thus, it is important to consider two potential
23 interpretations of this asymmetry.

24

25 Firstly, the possibility that hemispheric asymmetry exists for pathways that regulate sleep
26 cannot be ruled out since hemispheric asymmetry is often reported for other functions such as
27 right hemispheric dominance for attention (Hellman & Van Den Bell, 1980; Shulman et al.,
28 2010) or left hemispheric dominance for language (Knight et al., 2000). However, there is no
29 theoretical background to suggest that circuitry that regulates sleep should be lateralised.

30 Therefore, it cannot be concluded based on our data alone that the role of autonomic
31 projections from the suprachiasmatic nucleus in regulating daytime alertness is exclusive to
32 the left hemisphere.

33

1 Secondly, our data begs the question of why microstructure (FA) in the left hemisphere
2 predicts daytime sleepiness. The connection between the suprachiasmatic nucleus and the
3 lateral medulla passed through the region of locus coeruleus, which transmits ascending
4 noradrenergic projections that stimulate wakefulness as part of the reticular activating system
5 (Sapper et al., 2005). However, since microstructure (FA) predicted increased daytime
6 sleepiness rather than arousal, it is unlikely that the dissected pathway formed part of the
7 reticular activating system. This provides supporting evidence that the dissected pathway
8 instead forms part of descending sympathetic projections that trigger sleep inducing
9 melatonin secretion, thereby accounting for daytime sleepiness. However, our data did not
10 support our prediction that microstructure correlates with salivary measures of circadian
11 melatonin fluctuation. Therefore, while our data supports the hypothesis that the dissected
12 connection between the suprachiasmatic nucleus and the lateral medulla plays a role in sleep-
13 wakefulness cycles, it does not confirm the hypothesis that this pathway is involved in
14 regulation of circadian melatonin secretion. Future research may confirm laterality
15 differences in suprachiasmatic nucleus-lateral medulla pathway microstructure (FA) as
16 predictor of daytime sleepiness.

17

18 One major advantage of DTI tractography over other techniques is that it is a non-invasive
19 method for investigating white matter pathways in the brain. When using probabilistic DTI, it
20 is possible to make judgements on the reliability of the pathways observed (Parker, 2011),
21 and to compare factors that support the existence of a pathway (e.g. high FA value).
22 Therefore, probabilistic DTI is not only a quality assurance tool, but additionally allows for
23 comparison of white matter structural connectivity between brains from different groups of
24 individuals (Parker, 2011). The main contribution of this study is that the sympathetic
25 circadian pathways reported in humans, compares well with that found in the rat brain,
26 pointing to an anatomical representation of the human sympathetic circadian pathway.

27

28 Our data presents the first evidence that hypothalamic projections to the sympathetic nervous
29 system in humans play a role in regulating daytime sleepiness. The finding that daytime
30 sleepiness correlated strongly with microstructure (FA) of the streamline was not predicted
31 by our hypothesis; and certainly we had no basis to hypothesize lateralization of the effect to
32 the left hemisphere. Melatonin per se is not sedating in physiological amounts and its role is
33 to trigger sleep. Sleep is induced by the resulting serotonergic projection from the midline
34 raphe in the brainstem. The streamline virtually dissected in this investigation corresponds to

1 the dorsal longitudinal fasciculus of Schütz and is not consistent with projections from raphe
2 nuclei of the reticular activating system. Moreover, the microstructure (FA) of the streamline
3 did not correlate with melatonin levels. We are not, therefore, able to proffer a putative
4 mechanism accounting for the correlation between microstructure (FA) of the streamline and
5 daytime sleepiness. Nor can we offer an explanation for its laterality to the left hemisphere.
6 We can only conclude that the strong correlation between microstructure and behaviour
7 offers evidence for the veracity of the streamline as a functional anatomical pathway; and
8 suggest that the dorsal longitudinal fasciculus contains projections, in the left hemisphere,
9 that predict daytime sleepiness. We hope that our empirical findings will stimulate research
10 that will ultimately elucidate the physiological mechanisms involved.

11

12 **Conclusions**

13 Our data shows that daytime sleepiness, but not circadian rhythms, correlated with
14 microstructure of a brainstem sleep pathway connecting the suprachiasmatic nucleus and
15 lateral medulla, providing the first evidence for a functional role of hypothalamic projections
16 to the sympathetic nervous system in humans in sleep regulation.

17

18

19 **Disclosure/Conflict of Interest Statement**

20

21 The authors declare that the research was conducted in the absence of any commercial or
22 financial relationships that could be construed as a potential conflict of interest.

23

1 **References**

2
3
4
5
6
7
8
9
10
11
12
13
14
15
16
17
18
19
20
21
22
23
24
25
26
27
28
29
30
31
32
33
34

Alarma-Estrany, P., & Pintor, J. (2007). Melatonin receptors in the eye: location, second messengers and role in ocular physiology. *Pharmacol. Ther.* 113(3), 507-522.

Azadbakht H, Parkes LM, Haroon HA, Augath M, Logothetis NK, de Crespigny A, D'Arceuil HE, Parker GJM. (2015). Validation of high-resolution tractography against in vivo tracing in the macaque visual cortex. *Cereb Cortex*. First published March 18, 2015; doi:10.1093/cercor/bhu326.

Behrens, T. E. J., Woolrich, M. W., Jenkinson, M., Johansen-Berg, H., Nunes, R.G., Clare, S., Matthews, P. M., Brady, J. M. and Smith, S. M. (2003). Characterization and propagation of uncertainty in diffusion-weighted MR imaging. *Magn. Reson. Med.*, 50 (5), 1077-88.

Behrens, T. E. J., Berg, H. J., Jbabdi, S., Rushworth, M. F. S., & Woolrich, M. W. (2007). Probabilistic diffusion tractography with multiple fibre orientations: What can we gain? *Neuroimage*, 34(1), 144-155.

Beck, A. T., Steer, R. A., & Brown, G. K. (1996). Beck depression inventory-II. *San Antonio, TX*, 78204-2498.

Buijs, R. M., Wortel, J., Van Heerikhuizen, J. J., Feenstra, M. G. P., Ter Horst, G. J., Romijn, H. J. & Kalsbeek, A. (1999). Anatomical and functional demonstration of a multisynaptic suprachiasmatic nucleus adrenal (cortex) pathway. *Eur. J. Neurosci.* 11,1535–44.

Cechetto, D.F. & Saper, C.B. (1988) Neurochemical organization of the hypothalamic projection to the spinal cord in the rat. *Journal of Computational Neurology*, 272, 579–604.

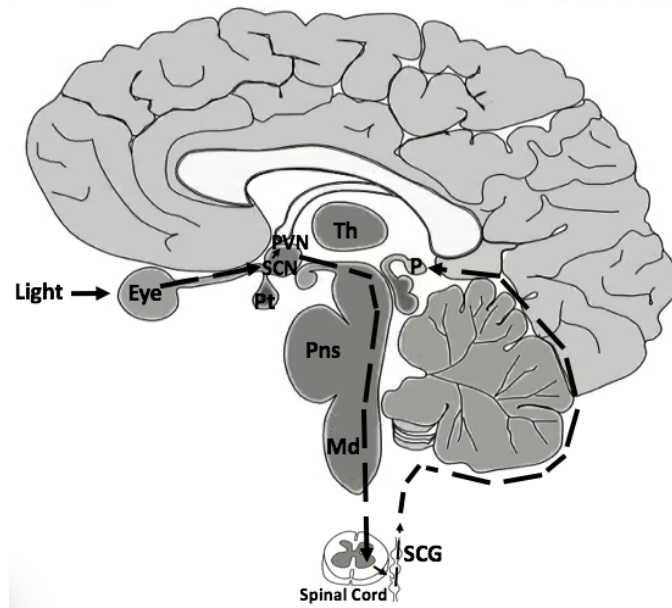
Fuller, A. & Fuller, C. (2002). *Circadian rhythms* In Encyclopedia of human brain Volume 1, California: Elsevier Sciences (USA).

Gooley, J. J., Lu, J., Chou, T. C., Scammell, T. E., & Saper, C. B. (2001). Melanopsin in cells of origin of the retinohypothalamic tract. *Nature Neurosci.* 4(12), 1165-1165.

1 Heilman, K. M., & Van Den Abell, T. (1980). Right hemisphere dominance for attention The
2 mechanism underlying hemispheric asymmetries of inattention (neglect). *Neurology*, 30(3),
3 327-327.
4
5 Hofman, M. A & Swaab, D. F. (1993). Diurnal and seasonal rhythms of neuronal activity in
6 the suprachiasmatic nucleus of humans. *J. Biol. Rhythms*, 8, 283–295.
7
8 Hoffstra, W. A. & De Weerd, A. W. (2008). How to assess circadian rhythm in humans: a
9 review of literature. *Epilepsy and Behav.* 13, 438-444.
10
11 Horne, J. A. & Östberg, O. (1976). A self-assessment questionnaire to determine
12 morningness-eveningness in human circadian rhythms. *Int. J Chronobiol.* 4, 97-100.
13
14 Hosoya, Y., Sugiura, Y., Okado, N., Loewy, A.D. & Kohno, K. (1991). Descending input
15 from the hypothalamic paraventricular nucleus to sympathetic preganglionic neurons in the
16 rat. *Exp. Brain Res.* 85, 10–20.
17
18 Johns, M. W. (1991). A new method for measuring daytime sleepiness: the Epworth
19 sleepiness scale. *Sleep*, 14 (6), 540–5.
20
21 Kappers, J. A. (1960). The development, topographical relations and innervation of the
22 epiphysis cerebri in the albino rat. *Z. Zellforsch. Microsk. Anat. Histochem.* 52, 163–215.
23
24 Kiernan JA (2005) *Barr's The Human Nervous System: An Anatomical Viewpoint.* 8th
25 Edition Lippincott Williams and Watkins
26
27 Knecht, S., Dräger, B., Deppe, M., Bobe, L., Lohmann, H., Flöel, A., & Henningsen, H.
28 (2000). Handedness and hemispheric language dominance in healthy
29 humans. *Brain*, 123(12), 2512-2518.
30
31 Larsen, P. L., Enquist, L. W., & Card, J. P. (1998). Characterization of the multisynaptic
32 neuronal control of the rat pineal gland using viral transneuronal tracing. *Eur. J. Neurosci.*
33 10, 128-14.
34

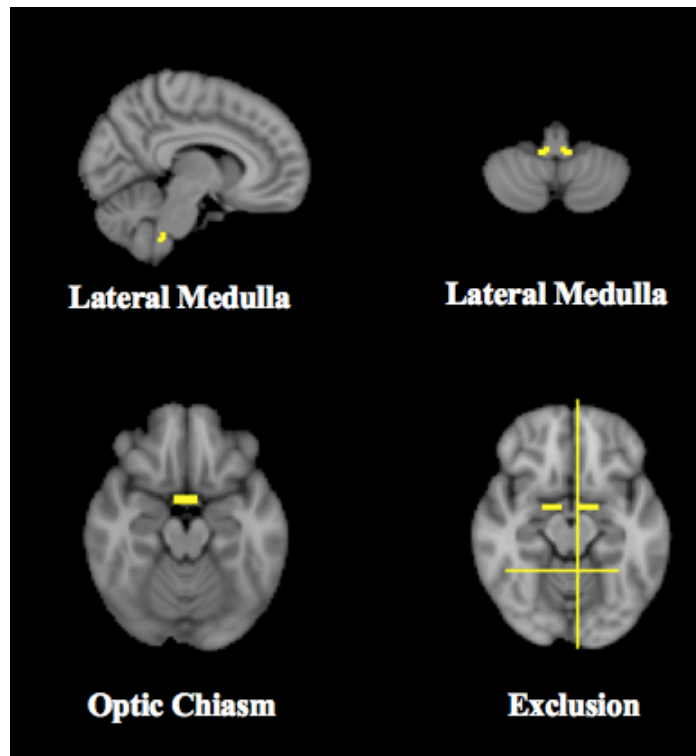
1 Larsen, P.J., Møller, M. & Mikkelsen, J.D. (1991). The intracerebral course of hypothalamic
2 paraventricular efferents involved in the regulation of pineal gland activity. *Adv. Pineal Res.*
3 5, 25–30.
4
5 Moore, R., Heller, A. & Wurtman, R. (1966). Visual pathway mediating pineal response to
6 environmental light. *Science*, 155, 220-223.
7
8 Moore, R. Y. & Card, J. P. (1986) Visual pathways and the entrainment of circadian rhythms.
9 *Ann. N. Y. Acad. Sc.* 453,123–133.
10
11 Naidich TP, Duvernoy HM, Delman BN, Sorensen, A. G., Kolia, S. S. & Haacke, M.
12 (2009). Duvernoy's Atlas of the Human Brain Stem and Cerebellum. Springer: Wien.
13
14 Parker, G.J.M. (2011). Probabilistic Fiber Tracking. In D. K. Jones, *Diffusion MRI: Theory,*
15 *Methods and Applications*, (pp.396-407). Oxford: Oxford University Press.
16
17 Saper, C. B., Scammell, T. E., & Lu, J. (2005). Hypothalamic regulation of sleep and
18 circadian rhythms. *Nature*, 437(7063), 1257-1263.
19
20 Shulman, G. L., Pope, D. L., Astafiev, S. V., McAvoy, M. P., Snyder, A. Z., & Corbetta, M.
21 (2010). Right hemisphere dominance during spatial selective attention and target detection
22 occurs outside the dorsal frontoparietal network. *J. Neurosci.* 30(10), 3640-3651.
23
24 Schütz (1891). Anatomische untersuchen uber den Faserverlauf im Zentralen Hohlengrau und
25 den nervenfaserschwund im Deselben bei der Progissiven Paralyse der.Ihren *Arch. f Psychiat.*
26 *Nervenkr.* 22: 526-616.
27
28 Swanson LW (1977) Immunohistochemical evidence for a neurophysin-containing
29 autonomic pathway arising in the paraventricular nucleus of the hypothalamus. *Brain*
30 *Research* 128(2):346–353.
31
32 Teclemariam-Mesbah, R., Ter Horst, G. J., Postema, F., Wortel, J. & Buijs, R.
33 (1999).Anatomical demonstration of the suprachiasmatic nucleus-pineal pathway. *J Comp.*
34 *Neurol.* 406,171–182.

1



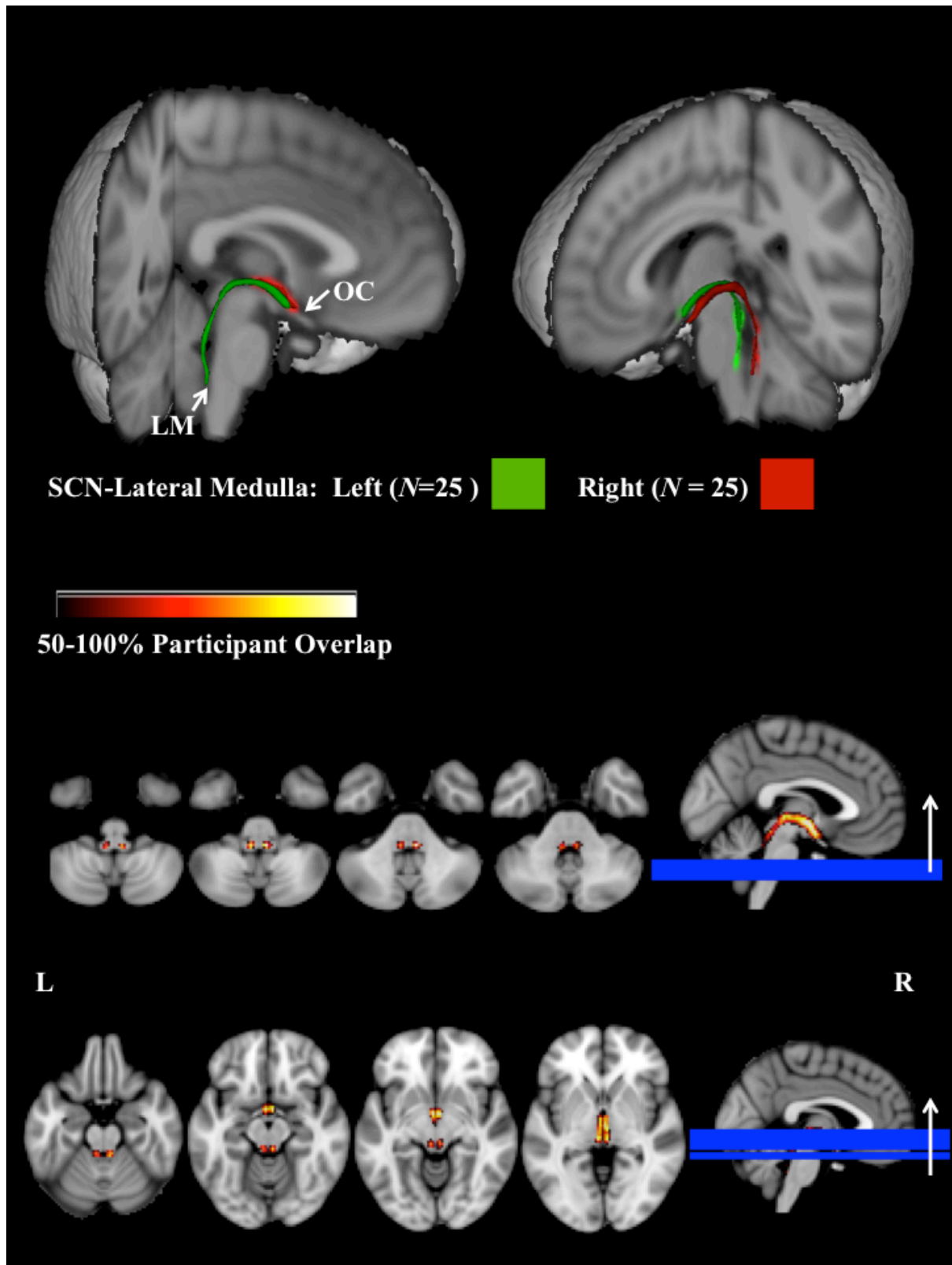
2

3 Figure 1. Multi-synaptic pathway from the suprachiasmatic nucleus to the pineal gland
4 regulating light induced melatonin inhibition. Light signals are transduced by melanopsin-
5 containing retinal ganglion cells in the eye and transmitted to the following structures in
6 order: the suprachiasmatic nucleus (SCN), the paraventricular nucleus (PVN), the
7 intermediolateral column of the thoracic spinal cord (via the lateral medulla) and the superior
8 cervical ganglion, terminating in the pineal gland.



1
2
3
4
5
6
7
8
9
10
11
12
13
14

Figure 2. Region of interest masks used to virtually dissect connection between the suprachiasmatic nucleus and lateral medulla. Examples of lateral medulla masks are shown in the coronal (top left) and saggital (top right) planes. Optic chiasm masks are demonstrated in the axial plan (bottom left). An exclusion mask was used during dissection of all tracts and is shown in the axial plane (bottom right). The exclusion mask included regions that would ensure exclusion of the optic radiations, cerebellum and a cross over of connections towards the opposite hemisphere. Due to the close proximity of central descending pathways in the brain stem, the mid-saggital exclusion midline region was drawn either slight left or slight right, depending on the hemisphere in which the tract was dissected, in order to avoid exclusion of the entire tract. For example, the mid-saggital exclusion region represented in the bottom left above was used as exclusion to dissect tracts in the left hemisphere.



1
2

3 **Figure 3.** Probabilistic tractography between the suprachiasmatic nucleus and the lateral
4 medulla ($N = 25$). Top: Composite 3D reconstruction of tracts in the left (shown in green)
5 and right (shown in red) hemispheres across all participants, aligned to the Montreal

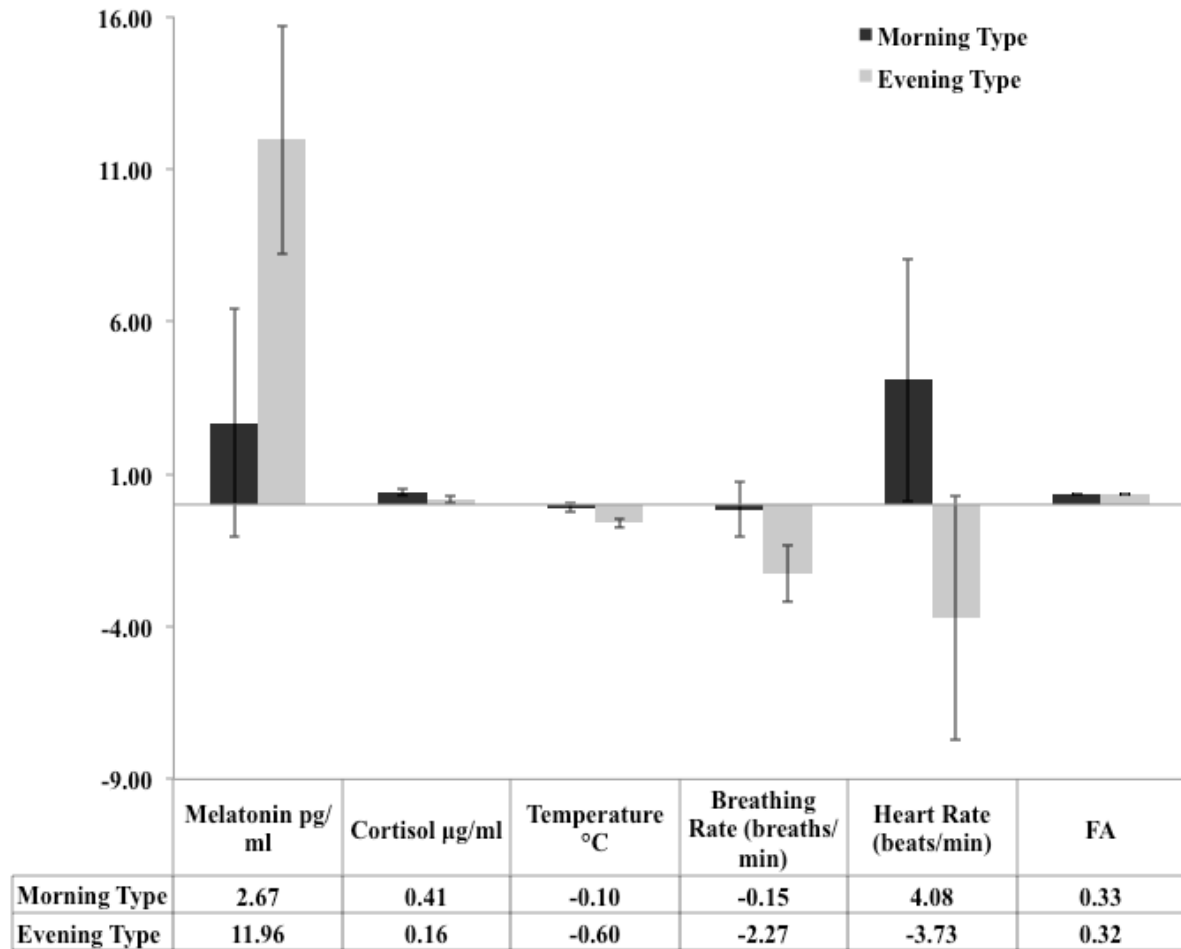
1 Neurological Institute T1-weighted standard brain. The composite connection was generated
2 by adding connections of all participants together, and was thresholded to include only voxels
3 that were common to connections in at least 75% of participants. Bottom: Composite tracts
4 connecting suprachiasmatic nucleus-lateral medulla shown in consecutive inferior to superior
5 axial slices. A lower threshold was used to include voxels that were common to connections
6 in at least 50% of participants to demonstrate variability across participants.

7
8
9
10
11
12
13
14
15
16
17
18
19
20
21
22
23
24
25
26
27
28
29
30
31
32

1 **Table 1.** Fractional anisotropy (FA) values for suprachiasmatic nucleus-lateral medulla
 2 connections in the left and right hemispheres across morning and evening types of
 3 individuals. Participant 9 was excluded due to failure to experiment instructions.

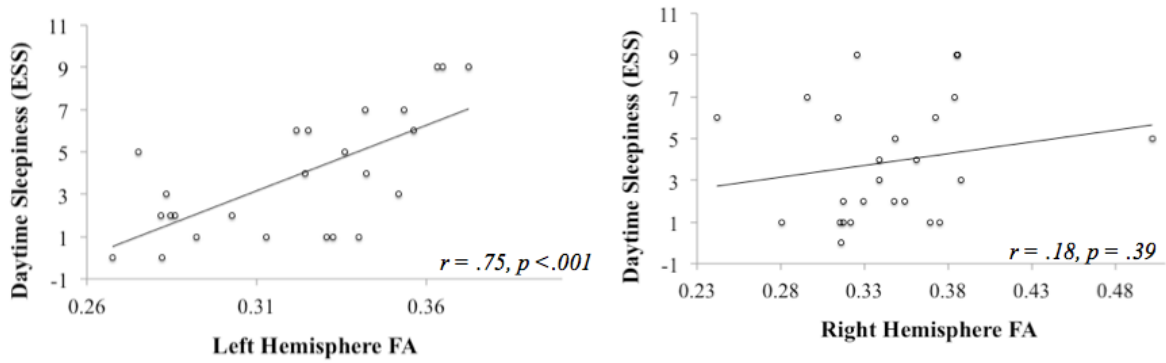
Participant	MEQ Type	Left Tract	Right Tract
1	Definite Morning	0.36	0.37
2	Definite Morning	0.32	0.34
3	Moderate Morning	0.30	0.35
4	Definite Morning	0.31	0.32
5	Moderate Evening	0.27	-
6	Definite Evening	0.28	0.39
7	Definite Evening	0.33	0.24
8	Definite Morning	0.37	0.39
10	Moderate Morning	0.33	0.32
11	Definite Evening	0.35	0.38
12	Definite Morning	0.28	0.33
13	Definite Evening	0.29	0.32
14	Definite Morning	0.36	0.33
15	Moderate Morning	0.28	0.32
16	Moderate Morning	0.34	0.50
17	Definite Evening	0.28	0.35
18	Definite Evening	0.36	0.39
19	Definite Evening	0.32	0.31
20	Definite Evening	0.35	0.34
21	Moderate Morning	-	0.38
22	Definite Morning	0.28	0.35
23	Moderate Evening	0.34	0.30
24	Moderate Morning	0.34	0.36
25	Definite Morning	0.33	0.37
26	Moderate Morning	0.29	0.32
27	Moderate Morning	0.34	0.28
Average		0.32	0.34

4



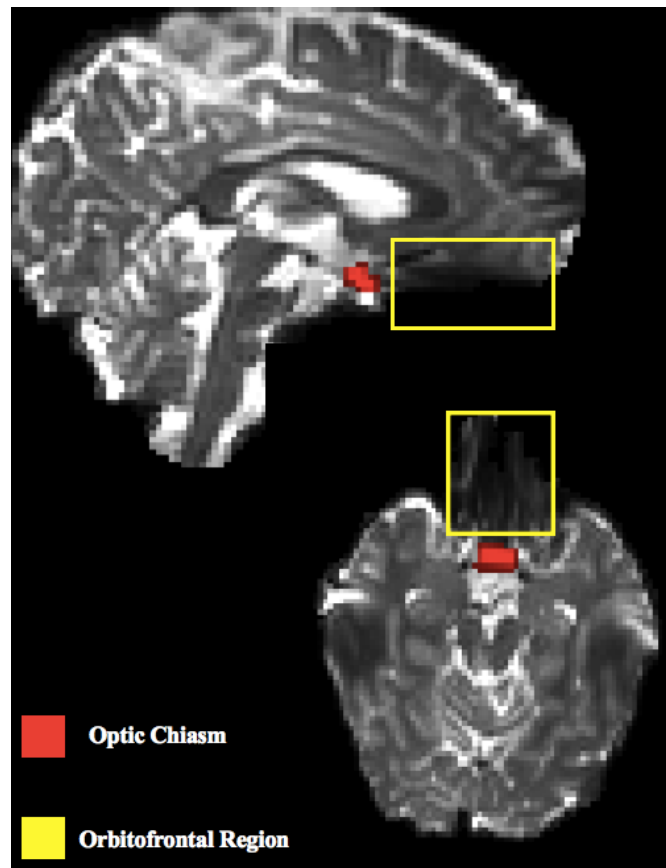
1
2
3
4
5
6
7
8
9
10
11
12
13

Figure 4. Bar graphs demonstrating diurnal differences in measures of melatonin, cortisol, temperature, breathing rate and mean fractional anisotropy (FA) of the suprachiasmatic nucleus-lateral medulla connection between morning and evening type groups of individuals. Difference scores for melatonin, cortisol, temperature, breathing rate and heart rate were calculated by subtracting scores collected in the evening from scores collected in the morning. Therefore, for example, a positive value of melatonin in the evening type group indicates higher melatonin scores in the morning compared to the evening for evening types. A negative score indicates lower scores in the morning compared to the evening measure. Error bars represent standard error of the mean. Independent samples t-tests demonstrated a significantly larger difference only for temperature ($t(23) = 2.58, p = .017$), however this effect did not survive Bonferroni correction for multiple comparisons.



1 **Figure 5.** Correlation scatterplot demonstrating microstructure (FA) of suprachiasmatic
 2 nucleus-lateral medulla connection in the left hemisphere (left) predicted daytime sleepiness
 3 as measured by the Epworth Sleepiness Scale (Johns, 1991).

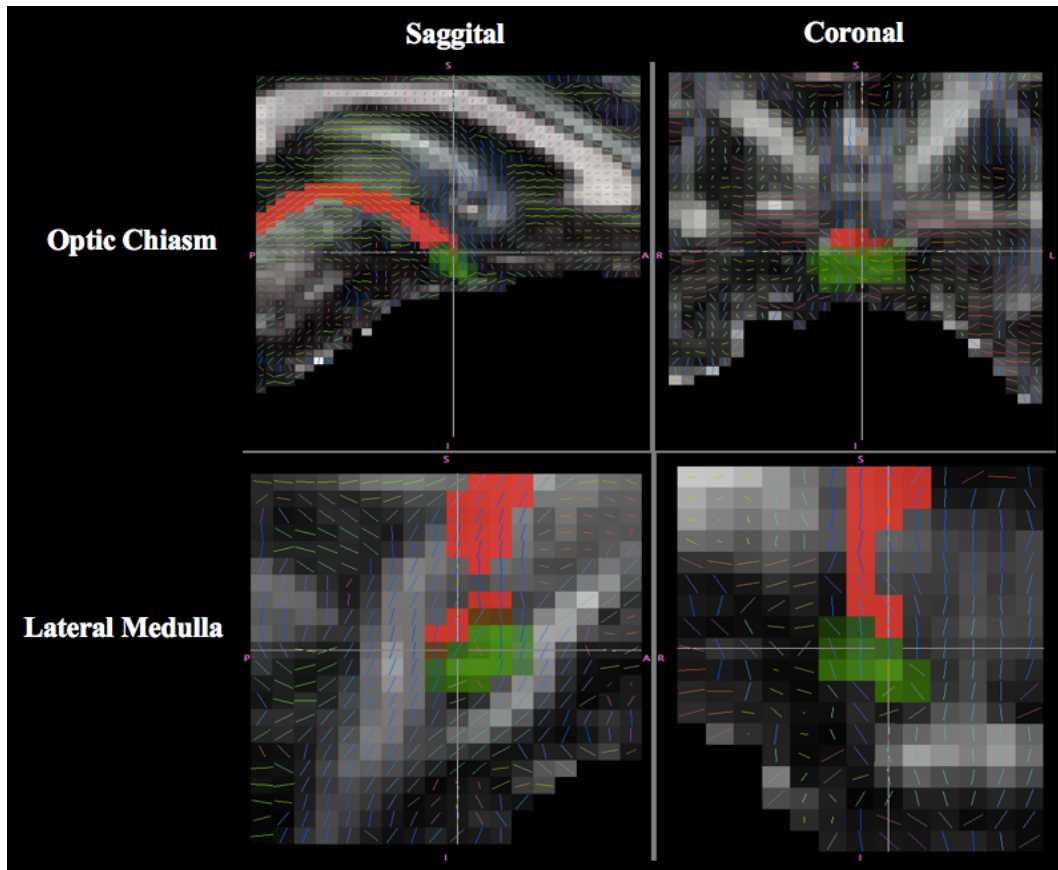
4
5



6
 7 **Figure 6.** The figure above illustrates a non-diffusion (B0) image from one representative
 8 participant, with the optic chiasm and orbito-frontal cortex regions marked for comparison of
 9 distortions. As is seen on the image, the region affected marked with a yellow box shows dark
 10 distortion, not affecting the optic chiasm (marked with red mask).

11

1



2

3 **Figure 7.** Close up illustration of tract (red) near the seed regions (green) in one representative
4 subject (top: optic chiasm mask in green; bottom: lateral medulla mask in green; sleep tract in
5 red. Note that the crosshairs highlight a voxel where the tract and mask overlap). As
6 demonstrated, it can be seen that the direction in each voxel along the tract follow along a
7 consistent trajectory. This can be clearly seen especially in the brainstem. The FA values are
8 lower ($\sim .2-.4$), as expected, in regions where the streamline passes through gray matter in the
9 mid-brain and medulla and higher as the tract passes through the brainstem and pons ($\sim .5$).

10